Molecular Therapy
Nucleic Acids
Original Article

# Triptolide Restores Autophagy to Alleviate Diabetic Renal Fibrosis through the miR-141-3p/PTEN/Akt/mTOR Pathway

Xiao-yu Li,[1] Shan-shan Wang,[1] Zhe Han,[1] Fei Han,[1] Yun-peng Chang,[1] Yang Yang,[1] Mei Xue,[1] Bei Sun,[1] and Li-ming Chen[1]

[1]Key Laboratory of Hormones and Development (Ministry of Health), Tianjin Key Laboratory of Metabolic Diseases, Tianjin Metabolic Diseases Hospital and Tianjin Institute of Endocrinology, Tianjin Medical University, Tianjin 300070, China

**Fibrosis is the major pathological feature of diabetic kidney disease (DKD). Autophagy, a process to maintain metabolic homeostasis, is obviously inhibited in DKD. Triptolide (TP) is a traditional Chinese medicine extract known for immune suppression and anti-inflammatory and anti-cancer activities. In this study, we investigated the effects of TP on autophagy and fibrosis in DKD. TP restored autophagy and alleviated fibrosis in DKD rats and high-glucose-incubated human mesangial cells. After we applied 3-methyladenine (an autophagy inhibitor) and autophagy-related gene 5-small interfering RNA (siRNA), we found that the improvement of fibrosis on TP was related to the restoration of autophagy. In addition, miR-141-3p levels were increased under high glucose but reduced after TP treatment. miR-141-3p overexpression aggravated the fibrosis and restrained the autophagy further, while miR-141-3p inhibition imitated the effects of TP. As an action target, phosphatase and tensin homolog (PTEN) showed corresponding opposite changes. After PTEN-siRNA transfection, the effects of TP on autophagy and fibrosis were inhibited. PTEN levels were downregulated, with downstream phosphorylated protein kinase B (Akt) and the mammalian target of rapamycin (mTOR) upregulated in high glucose, which were reversed by TP treatment. These findings indicate that TP alleviates fibrosis by restoring autophagy through the miR-141-3p/PTEN/Akt/mTOR pathway and is a novel therapeutic option for DKD.**

## INTRODUCTION

With the prevalence of diabetes mellitus (DM) rising dramatically, concomitant diabetic kidney disease (DKD) has considerably influenced the long-term quality of life of patients with diabetes.[1,2] In the beginning, DKD has several silent phases that cannot be clinically measured, such as glomerular hyperfiltration and hyperperfusion. Subsequently, morphological changes occur, including thickening of the glomerular basement membrane, glomerular hypertrophy, mesangial expansion, and expansion of the tubulointerstitium. As DKD progresses, patients experience microalbuminuria, proteinuria, hypertension, and even renal failure.[2] Fibrosis is one of the major pathologic changes in DKD, which is caused by aggregation of extracellular matrix (ECM), including type IV collagen (Col IV) and fibronectin (FN). Unfortunately, there are not enough effective treatments for DKD.

Autophagy is a conserved process to maintain intracellular metabolic homeostasis, accompanied by a landmark double-membrane structure called the autophagosome. The cellular components are confined in autophagosomes and subsequently degraded by lysosomes. Autophagy initiates in response to hypoxia, light, starvation, DNA damage, and so on.[3–6] Changes in autophagy are detected by microtubule-associated protein 1 light chain 3 (LC3) and sequestosome 1 (SQSTM1/P62). LC3, located on the autophagosomal membrane, consists of cytosolic LC3 I and membrane-bound LC3 II. P62 is preferentially degraded by autophagy, and the inhibition of autophagy leads to an increase in P62 levels. In addition, autophagy-related genes (Atgs) are a group of autophagy-essential genes. Atg5 conjugates with Atg12 and Atg16 to mediate phosphatidylethanolamine (PE) lipidation of LC3 for expansion of the autophagosomal membrane. 3-methyladenine (3-MA) effectively blocks an early stage of autophagy by inhibiting the class III phosphoinositide 3-kinase (PI3K). Autophagy is deficient or insufficient in DKD and the restoration of autophagy may be a novel therapeutic option.[7] Research has shown that autophagy has obvious significance in ameliorating tubulointerstitial fibrosis, but study in glomerulus is very few.[8,9]

MicroRNAs (miRNAs) are a class of small non-coding RNAs that regulate gene expression by either downregulating mRNA levels or

Received 10 August 2017; accepted 22 August 2017;
http://dx.doi.org/10.1016/j.omtn.2017.08.011.

**Correspondence:** Li-ming Chen, Key Laboratory of Hormones and Development (Ministry of Health), Tianjin Key Laboratory of Metabolic Diseases, Tianjin Metabolic Diseases Hospital and Tianjin Institute of Endocrinology, Tianjin Medical University, 300070 Tianjin, China.
**E-mail:** xfx22081@vip.163.com
**Correspondence:** Bei Sun, Key Laboratory of Hormones and Development (Ministry of Health), Tianjin Key Laboratory of Metabolic Diseases, Tianjin Metabolic Diseases Hospital and Tianjin Institute of Endocrinology, Tianjin Medical University, 300070 Tianjin, China.
**E-mail:** sun_peipei220@hotmail.com

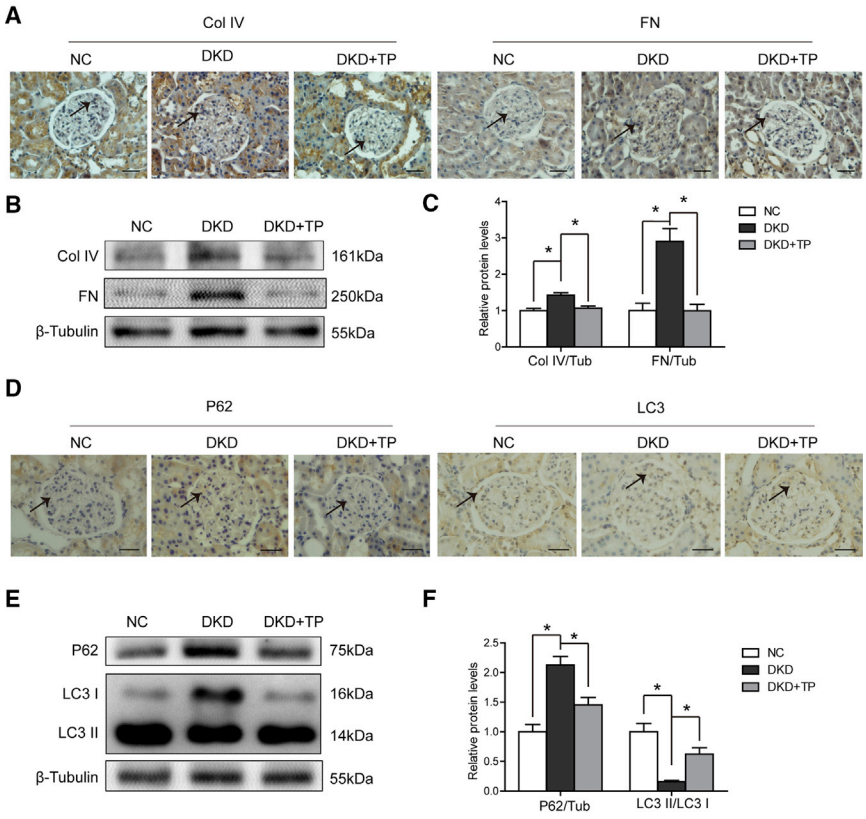


**Figure 1. TP Alleviated Hyperglycemia-Induced Fibrosis and Restored Autophagy in DKD Rats**

(A) Immunohistochemical staining of Col IV and FN in glomeruli of rats. Scale bars in the right lower corner represent 20 μm. (B) Representative western blot analysis of Col IV and FN in rats. (C) Densitometric results of Col IV and FN, as determined by western blot. Error bars represent SEM. (D) Immunohistochemical staining of P62 and LC3 in glomeruli of rats. Scale bars in the right lower corner represent 20 μm. (E) Representative western blots of P62 and LC3 in DKD rats. (F) Densitometric results of P62 and LC3, as determined by western blot. Error bars represent SEM. DKD, diabetic kidney disease; NC, normal control; TP, triptolide. *$p < 0.05$.

directly repressing translation of genes. Many miRNAs are corrected with DKD, such as miR-21, miR-184, and miR-192, while there are few studies of miRNA on fibrosis or autophagy in DKD.[10–12] miR-141-3p is a member of the miR-200 family (miR-200a, 200b, 200c, 141, and 429), which is greatly involved in the therapy of cancer. The role of miR-141-3p in DKD is still unknown.

*Tripterygium wilfordii* Hook F (TWHF) is extracted from an ancient Chinese herb, *Tripterygium*. TWHF is generally used in the treatment of proteinuria in DKD and displays obvious adverse effects such as liver function impairment. Triptolide (TP) is one of the primary and active components of TWHF. As a pure compound, TP may provide a way to hedge the adverse effects. To date, researchers have identified the effects of TP on inflammation, cancer, the immune system, and diabetic cardiomyopathy.[13–16] However, there are relatively few studies on the effects of TP on DKD and TP's mechanism of action is still not clear and definite.

Phosphatase and tensin homolog on chromosome 10 (PTEN) regulates signal transduction pathways by both phosphatase-dependent and phosphatase-independent mechanisms. PTEN suppresses the activation of downstream phosphorylated protein kinase B (Akt)/mammalian target of rapamycin (mTOR), a master regulator of cellular metabolism. In this study, we explored the role of TP in autophagy and fibrosis, along with the possible mechanism involved in DKD. We speculated that TP could restore autophagy to alleviate fibrosis via the miR-141-3p/PTEN/Akt/mTOR pathway, resulting in the improvement of DKD.

## RESULTS

### Effects of TP on Autophagy and Fibrosis of DKD Rats

The results of immunohistochemistry staining (IHC) and western blot (WB) analysis showed changes in Col IV and FN between the negative control group (NC), the DKD group (DKD), and the DKD with TP treatment group (DKD+TP), respectively. In DKD, the accumulation of Col IV and FN on IHC was obviously increased in the glomeruli compared to that in NC (Figure 1A), which was also shown in WB analysis (Figure 1B). However, expression of Col IV and FN was extremely reduced in DKD+TP (Figures 1A and 1B). Expression of P62 increased in DKD but recovered in DKD+TP, both shown on IHC and WB (Figures 1D and 1E). Furthermore, the accumulation points of LC3 in IHC significantly decreased in the glomeruli and the ratio of LC3 II to LC3 I in WB reduced in the DKD group, meaning the autophagy was inhibited in DKD. On the other hand, TP rescued LC3 aggregation and the ratio of LC3 II to LC3 I was restored in DKD+TP (Figures 1E and 1E). TP reversed the effects of autophagy and fibrosis in DKD rats.

### Effects of TP on Autophagy and Fibrosis of Human Mesangial Cells

We confirmed the effects of TP on autophagy and fibrosis with human mesangial cells (HMCs) as well. Immunofluorescence (IF) results showed that Col IV and FN expression was increased in cells after high glucose (HG) treatment, while it was reduced in the HG and TP treatment group (HG+TP; Figure 2A). In addition, changes in P62 and LC3 were explored with confocal IF microscopy. As shown in Figure 2D, P62 levels were significantly increased in HG but were restored in HG+TP. Punctate LC3 points were decreased in HG but

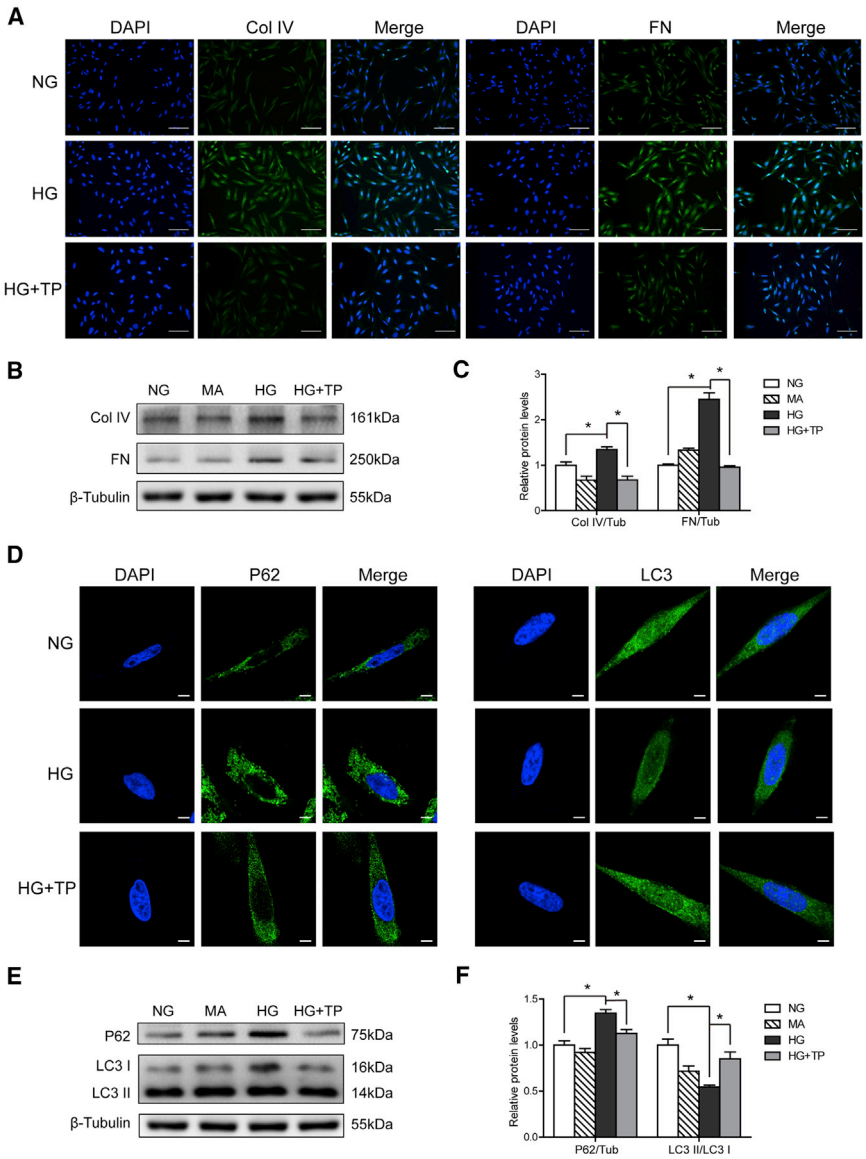


**Figure 2. TP Alleviated High-Glucose-Induced Fibrosis and Restored the Autophagy of HMCs**

(A) Immunofluorescence of Col IV and FN in HMCs. Scale bars in the right lower corner represent 50 μm. (B) Representative western blot analysis of Col IV and FN in HMCs. (C) Densitometric results of Col IV and FN, as determined by western blot. Error bars represent SEM. (D) Immunofluorescence of P62 and LC3 in HMCs. Scale bars in the right lower corner represent 5 μm. (E) Representative western blots of P62 and LC3 in HMCs. (F) Densitometric results of P62 and LC3, as determined by western blot. Error bars represent SEM. HG, high glucose; MA, mannitol; NG, normal glucose; TP, triptolide. *$p < 0.05$.

increased in HG+TP (Figure 2D). We also proved the results with WB (Figure 2B and 2E). Results at protein levels were the same as the consequences of IF. Furthermore, there was no significant difference between mannitol (MA) and normal glucose (NG), excluding the interference of hyperosmosis.

Interestingly, autophagy was not inhibited at the beginning (Figure S1). P62 levels were decreased in HG compared to those in NG before 24 hr. After 24 hr, expression of P62 obviously increased, demonstrating that autophagy changed over time and varied bi-directionally. Furthermore, changes in cellular morphology were observed in the experiments (Figures 2A and 2D). Cells in NG presented as slender spindle cells. After treatment with HG, the shapes of cells and nuclei were both shorter and fatter. But the TP partly rescued the normal forms in HG-treated cells, implying the recovery of cellular morphology by TP.

### Alleviation of Fibrosis by TP Was Blocked by 3-MA and Atg5-siRNA

We applied Atg5-siRNA and 3-MA to explore the relationship between autophagy and fibrosis under HG and HG+TP. Compared to HG, the levels of P62, Col IV, and FN were all significantly upregulated in HG+3-MA, meaning that ECM accumulation was accelerated by 3-MA. TP weakened the enhancement in P62, Col IV, and FN in HG+TP, compared to HG, again demonstrating the function of TP on autophagy and fibrosis. In addition, we contrasted the protein levels in HG+TP with those in HG+TP+3-MA and discovered that the levels of P62, Col IV, and FN were increased in turn, indicating that the alleviation of fibrosis by TP was blocked by 3-MA and was autophagy related (Figures 3A and 3B). Similarly, after Atg5-siRNA transfection, autophagy was inhibited and the improved effect of TP on fibrosis was impaired (Figure 3C). All of these results indicate that TP relieved fibrosis through the regulation of autophagy.

### TP Affected Autophagy and Fibrosis under HG by miR-141-3p

We assumed that TP restored autophagy via miRNA. To determine the involved miRNA, we applied gene chip technology to detect the obviously changed miRNA. miR-141-3p was significantly increased in HG but reduced in HG+TP (Figure S2). Then we semi-quantified miR-141-3p in cells treated with NG, MA, HG, and HG+TP, respectively. We found that there were significant differences between NG and HG, but no obvious changes in miR-141-3p levels between NG and MA. Compared with HG, miR-141-3p showed a significant decrease in HG+TP (Figure 4A). Furthermore, we transfected cells with an miR-141-3p inhibitor (miR-141i),

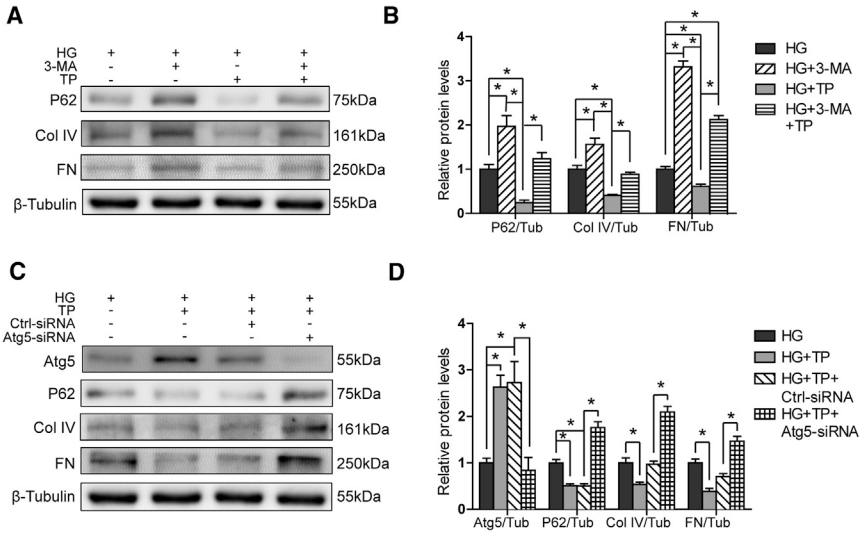


**Figure 3. The Attenuated Function of TP on Renal Fibrosis Was Related to Autophagy Upregulation**

(A) Representative western blots of P62, Col IV, and FN for different groups. (B) Densitometric results of P62, Col IV, and FN, as determined by western blot. Error bars represent SEM. (C) Representative western blots of Atg5, P62, Col IV, and FN for different groups. (D) Densitometric results of Atg5, P62, Col IV, and FN, as determined by western blot. Error bars represent SEM. 3-MA, 3-methyladenine; Atg5-siRNA, autophagy-related gene 5-siRNA; Ctrl-siRNA, siRNA negative control; HG, high glucose; TP, triptolide. *$p < 0.05$.

miR-141-3p mimics (miR-141 m), and a homologous negative control (NCi and NCm) to detect the influence of miR-141-3p on autophagy and fibrosis. P62, Col IV, and FN levels were significantly reduced in the HG+miR-141i group, and the ratio of LC3 II/LC3 I was significantly increased compared to the HG+NCi group (Figures 4B and 4C). Levels of P62, Col IV, and FN were significantly increased in HG+TP+miR-141 m compared to those in HG+TP+NCm (Figures 4D and 4E). Therefore, we considered that TP regulated the autophagy and fibrosis through miR-141-3p in HMCs.

### TP Regulated Autophagy and Fibrosis by the PTEN/Akt/mTOR Pathway

After we determined the role of miR-141-3p in autophagy and fibrosis, we exerted further efforts to determine the exact internal mechanism. We searched TargetScan (http://www.targetscan.org/vert_71/) to predict the miR-141-3p potential binding site. The 3′ UTR of PTEN matched the sequence of miR-141-3p exactly (Figure 5A). A dual-luciferase reporter system confirmed that PTEN was a direct target and miR-141 m significantly reduced the expression of PTEN, compared to NCm in the HMCs (Figure 5B). Cells were transfected with PTEN-siRNA to confirm the function of PTEN. The levels of P62, Col IV, and FN were significantly increased in HG+TP+PTEN-siRNA compared to those in HG+TP+Ctrl-siRNA (Figures 5C and 5D), demonstrating the involvement of PTEN in autophagy and fibrosis. Experiments later showed that PTEN levels in HG were obviously reduced, although they were regained after TP treatment (Figures 5E and 5F). In addition, downstream p-Akt and p-mTOR levels were significantly increased in HG but were restored in HG+TP (Figures 5E and 5F). Similarly, the restoration of TP on PTEN/Akt/mTOR was obviously suppressed after transfection with PTEN-siRNA (Figures 5G and 5H). All of these results implied that TP regulated autophagy and fibrosis through the PTEN/Akt/mTOR pathway.

### Function of TP on PTEN/Akt/mTOR Was Reversed by Overexpression of miR-141-3p

To further confirm that TP takes effect through the miR-141-3p/PTEN/Akt/mTOR pathway, we transfected HMCs with miR-141 m, miR-141i, NCi, and NCm again. The protein levels of PTEN were significantly increased after miR-141i transfection, and those of p-Akt and p-mTOR were significantly decreased (Figures 6A and 6B). On the contrary, after miR-141 m transfection, the protein levels of PTEN were obviously reduced but those of p-Akt and p-mTOR were significantly increased (Figures 6C and 6D), meaning that the function of TP on the PTEN/Akt/mTOR pathway was blocked by overexpression of miR-141-3p. These findings further determined that TP regulates autophagy and fibrosis through the miR-141-3p/PTEN/Akt/mTOR pathway.

## DISCUSSION

A large number of clinical trials have shown that TWHF can reduce proteinuria and serum creatinine levels in patients with DKD.[17,18] In spite of the valid therapeutic action on DKD, the adverse effects of TWHF were identically strong, including liver function impairment, menstrual disturbance, hyperkalemia, and reduction in the white blood cell count.[17,18] TP is shown to ameliorate proteinuria and renal injury by inhibiting inflammation and macrophage infiltration, reserving the therapeutic effects of *Tripterygium* glycosides on DKD.[19–22] Liver function impairment and hematologic toxicity did not occur in our study. The study on TP, a major active component isolated from TWHF, may contribute to the escape of toxicity of TWHF.

Renal mesangial cells provide structural support for the glomerulus and produce ECM. Col IV and FN progressively occlude the renal capillaries and damage the filtration unit in the kidney.[23] As shown in our study, mesangial cells evidently proliferate and produce excessive ECM, such as Col IV and FN, resulting in fibrosis in DKD. However, TP treatment could reduce the aggregation of ECM, relieve fibrosis, and delay progression of end-stage renal disease.

Fibrosis can be regulated through autophagy, a biological regulatory program that maintains homeostasis.[24] In our study, the degree of

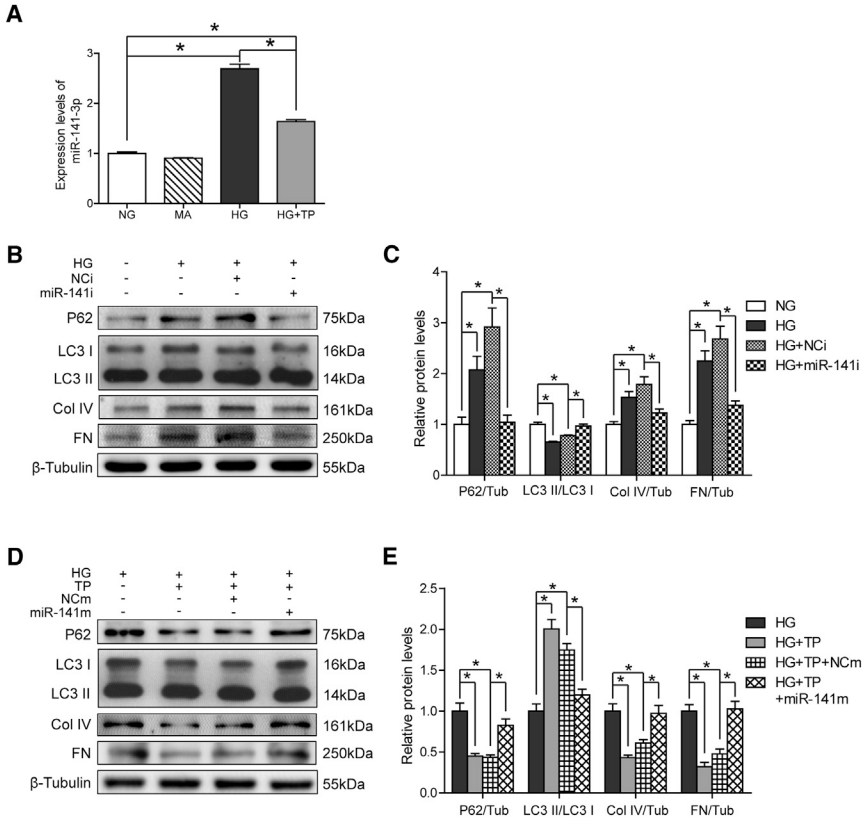


**Figure 4. TP Acted on Autophagy and Fibrosis through miR-141-3p**

(A) Differential expression of miR-141-3p in each group. The level of miR-141-3p expression is expressed relative to that of U6 snRNA. Error bars represent SEM. (B) Representative western blots of P62, LC3, Col IV, and FN for different groups. (C) Densitometric results of P62, LC3, Col IV, and FN, as determined by western blot. Error bars represent SEM. (D) Representative western blots of P62, LC3, Col IV, and FN for different groups. (E) Densitometric results of P62, LC3, Col IV, and FN, as determined by western blot. Error bars represent SEM. HG, high glucose; MA, mannitol; miR-141 m, miR-141-3p mimics; miR-141i, miR-141-3p inhibitor; NCi, miR-141-3p inhibitor control; NCm, miR-141-3p mimics control; NG, normal glucose; TP, triptolide. *p < 0.05.

fibrosis was aggravated after autophagy was suppressed by 3-MA and Atg5-siRNA. On the one hand, autophagy affects the levels of transforming growth factor β (TGF-β), a principle cytokine in renal fibrosis.[25] TGF-β stimulates fibrosis progression through the Smad, extracellular signal-regulated kinase (ERK), and p38-mitogen-activated protein kinase (MAPK) pathways, among others.[26–28] On the other hand, autophagy can directly prevent excess accumulation of collagen in the kidney.[29]

The levels of autophagy are reduced in DKD but are partially reversed by insulin injection and allogenic islet transplantation. In our study, bands of LC3II in WB results were more distinct than LC3 I, probably because LC3 I was more labile than LC3 II and was less sensitive to detection by antibodies. In addition, changes in LC3 II amounts were dependent on the tissue and cellular context.[30] Considering that we applied the ratio of LC3 II to LC3 I along with P62 (another marker for autophagy), we believe that the results for autophagy are reliable. Furthermore, we discovered that a short period of glucose stimulation induced autophagy activation, whereas prolonged glucose stimulation led to autophagy inhibition. It was consistent with the results using human renal proximal tubule epithelial cell lines (HK-2).[31] Regarding short-time glucose stimulation as an extracellular stress, autophagy reacts dynamically to serve as a protective response.[32] However, with prolonged reaction time, some specific cytokines and signals for HG are evoked and autophagy is inhibited.

Moreover, previous experiments show that TP can enhance autophagy in Parkinson's disease or prostate cancer.[33,34]

Three core pathways regulate autophagy: mTOR, AMP-activated protein kinase (AMPK), and sirtuins (SIRTs). In our study, TP restored autophagy by mTOR, regulated upstream by PTEN and Akt. As mentioned earlier, the levels of PTEN were reduced in HG but increased by TP. Loss of PTEN induces the accumulation of phosphatidylinositol-3,4,5-trisphosphate (PIP3) for its dephosphorylation at position 3 on the inositol ring.[35] Excessive PIP3 either directly activates Akt or indirectly phosphorylates Thr308 through 3-phosphoinositide-dependent kinase 1 (PDK1).[36,37] Akt activates mTORC1 through inhibition of tuberous sclerosis complex (TSC) 2, a GTPase-activating protein (GAP) toward the Ras homolog enriched in brain (Rheb) GTPase, which phosphorylates mTOR1.[38,39] Akt also phosphorylates and inhibits PRAS40, suppressing the phosphorylation of mTORC1.[40] mTOR is a serine/threonine protein kinase and consists of two functional complexes: mTORC1 and mTORC2. mTORC1 inhibits autophagy through direct regulation of the Unc-51-like kinase (ULK1)/Atg13/focal adhesion kinase family-interacting protein of 200 kDa (FIP200) complex, which is essential for autophagy initiation.[41] Moreover, mTORC1 prevents ULK1 activation by directly phosphorylating Ser757 to adjust autophagy.[42]

However, in this study, TP did not act on PTEN directly, but rather through the intermediary of miR-141-3p. miR-141-3p has shown modulatory effects on epithelial to mesenchymal transition (EMT), tumor metastasis, and oxidative stress response.[43–45] Changes in miR-141-3p might be downregulated in rat proximal tubule epithelial cells (NRK52E) treated with TGF-β but upregulated in mouse hearts modeled by low-dose streptozotocin (STZ) with a multiple injection method,[46,47] which is consistent with our results. Moreover, miR-141-3p levels were reduced in rats with unilateral ureteral obstruction

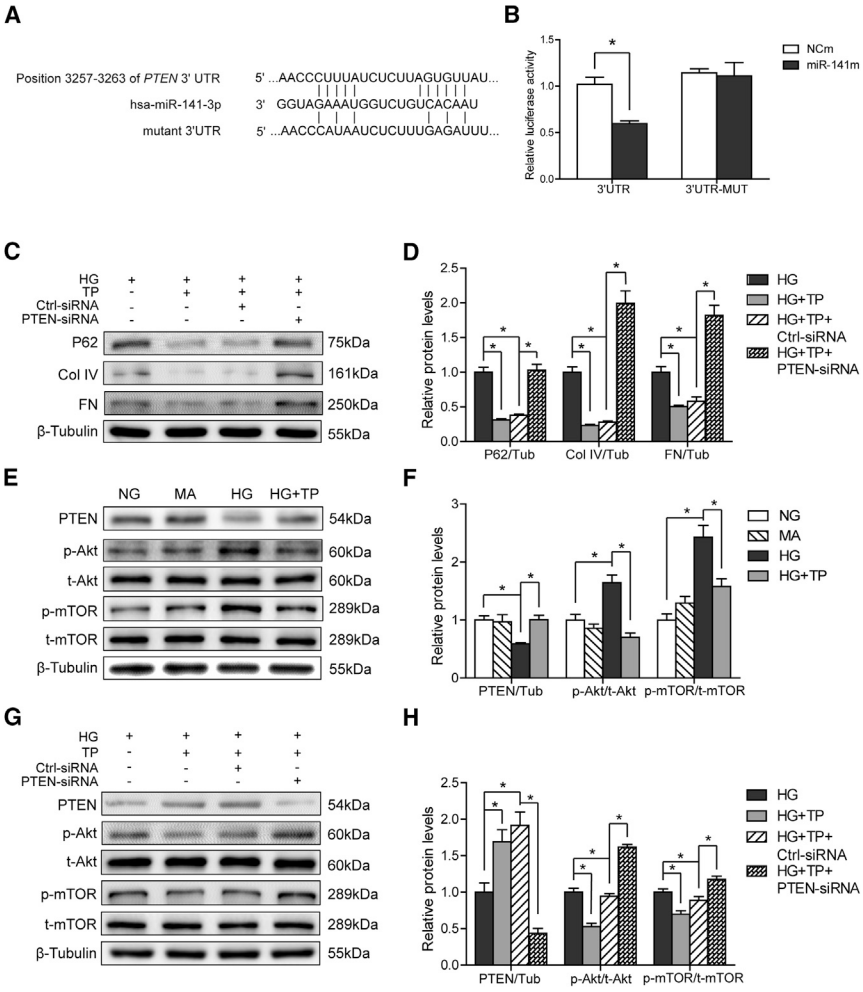


**Figure 5. TP Regulated Autophagy and Fibrosis by PTEN, One of miR-141-3p's Target Genes**

(A) Alignment of miR-141-3p with the predicted target region in the PTEN 3′ UTR. An interaction sequence among the wild-type PTEN 3′ UTR, miR-141-3p, and the mutant PTEN 3′ UTR construct is shown. (B) The luciferase reporter assay using HMCs showed the direct interaction between miR-141-3p and the 3′ UTR of PTEN. After 24 hr, miR-141 m reduced the ratio of Renilla-to-Firefly expression, but not when the 3′ UTR bore mutations at the miR-141-3p binding site. Error bars represent SEM. (C) Representative western blots of P62, Col IV, and FN for different groups after transfection with PTEN-siRNA. (D) Densitometric results of P62, Col IV, and FN, as determined by western blot. Error bars represent SEM. (E) Representative western blots of PTEN, p-Akt, t-Akt, p-mTOR, and t-mTOR for different groups. (F) Densitometric results of PTEN, p-Akt, t-Akt, p-mTOR, and t-mTOR as determined by western blot. Error bars represent SEM. (G) Representative western blots of PTEN, p-Akt, t-Akt, p-mTOR, and t-mTOR for different groups after transfection with PTEN-siRNA. (H) Densitometric results of PTEN, p-Akt, t-Akt, p-mTOR, and t-mTOR as determined by western blot. Error bars represent SEM. Ctrl-siRNA, siRNA negative control; HG, high glucose; MA, mannitol; miR-141 m, miR-141-3p mimics; NCm, miR-141-3p mimics control; NG, normal glucose; PTEN-siRNA, phosphatase and tensin homolog-siRNA; TP, triptolide. *$p < 0.05$.

(UUO).[48] It is well known that TGF-β stimulation and UUO are both classical models for renal interstitial fibrosis, and injection of STZ is a typical model for DM. We speculate that the levels of miR-141-3p increase in DM-induced pathologic changes but decrease in simple fibrosis models, which needs further validation.

## MATERIALS AND METHODS

### Animals

Six-week-old male Sprague-Dawley rats were purchased from HFK Bioscience Company (Beijing, China). All experimental rats were maintained in environmentally controlled animal facilities at Tianjin Medical University. All animal procedures were approved by the Tianjin Medical University Experimental Animal Ethics Committee. Rats (n = 36) were randomly assigned to 3 groups. Rats in the normal control group (n = 8) were fed a standard diet and the other rats were fed a high-fat diet (HFD) for 8 weeks. HFD-fed rats were injected intraperitoneally with a single dose of STZ (30 mg/kg; Sigma, MO, USA) in citrate buffer, while NC rats received an equal volume of citrate buffer. Glucose levels were detected 3 days after injection and 24-hr urine samples were collected in metabolic cages. Animals with random blood glucose levels ≥16.7 mM were regarded as diabetic (DM rats; n = 26). With the time prolonging, rats who had high blood glucose levels and 24-hr urinary microalbumin (UMA) levels ≥30 mg were considered to have DKD (n = 23). Then 11 diabetic rats were randomly chosen to receive treatment with TP (200 μg/kg/d) as the DKD+TP group (n = 11). Other DKD rats (n = 12) and NC rats (n = 8) were offered an equal volume of saline. The liquid was distributed by daily gastric gavage for 12 weeks. Physical and biochemical parameters of the rats are listed in Table S1.

### Cell Culture

HMCs were obtained from American Type Culture Collection (ATCC; USA). The cells were cultured in 1640 medium (Gibco, MA, USA), containing 5% fetal bovine serum (Biolnd, Israel), 100 U/mL penicillin, and 100 U/mL streptomycin at 37°C and 5% $CO_2$. All cells were incubated serum free for 6–8 hr before treatment for synchronization. Then the cells were divided as follows: cells from the NG group were incubated in 1640 with 5.5 mM glucose, (2) cells from the MA group were incubated in 1640 with 5.5 mM glucose and 19.5 mM MA, (3) cells from the HG group were incubated in 1640 with 25 mM glucose, and (4) cells from the TP intervention group (HG+TP) were incubated in 1640 with 25 mM glucose and 10 μM TP (National Institute for the Control of Pharmaceutical and Biological Products, Beijing, China) for 48 hr. The TP concentration was

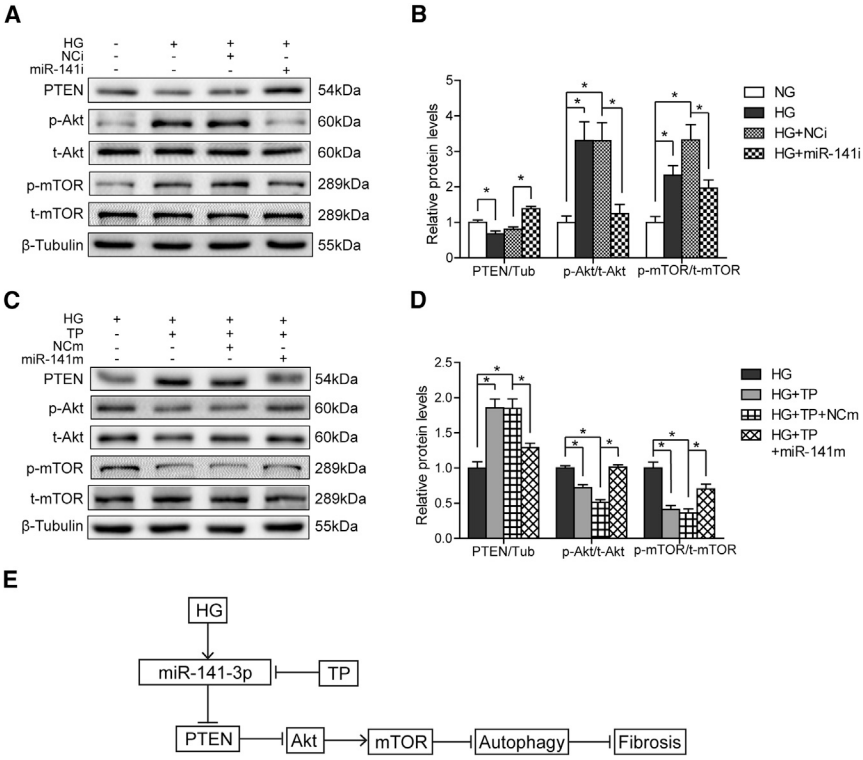


**Figure 6. TP Regulated Autophagy and Fibrosis through the miR-141-3p/PTEN/Akt/mTOR Pathway**

(A) Representative western blots of PTEN, p-Akt, t-Akt, p-mTOR, and t-mTOR for different groups. (B) Densitometric results of PTEN, p-Akt, t-Akt, p-mTOR, and t-mTOR as determined by western blot. Error bars represent SEM. (C) Representative western blots of PTEN, p-Akt, t-Akt, p-mTOR, and t-mTOR for different groups. (D) Densitometric results of PTEN, p-Akt, t-Akt, p-mTOR, and t-mTOR as determined by western blot. Error bars represent SEM. (E) TP suppresses the upregulated miR-141-3p, acting at the PTEN/Akt/mTOR pathway to restore autophagy, which could attenuate fibrosis in DKD. HG, high glucose; miR-141 m, miR-141-3p mimics; miR-141i, miR-141-3p inhibitor; NCi, miR-141-3p inhibitor control; NCm, miR-141-3p mimics control; NG, normal glucose; TP, triptolide. *$p < 0.05$.

selected based on the results of a Cell Counting Kit 8 (CCK8) assay (Figure S3).

### WB

Cell protein and rats' renal protein were extracted in RIPA lysis buffer with PMSF, phosphatase inhibitors, and loading buffer. Equal amounts of protein samples were loaded on SDS-PAGE and then transferred onto polyvinylidene fluoride (PVDF; Millipore, MA, USA) membrane. After blocking in milk for 2 hr, the membranes were incubated with primary antibodies against SQSTM1/P62 (1:1,000; Abcam, MA, USA), LC3 (1:1,000; CST, MA, USA), Col IV (1:500; Proteintech, IL, USA), FN (1:1,000; Proteintech, IL, USA), Atg5 (1:1,000; CST, MA, USA), PTEN (1:1,000; CST, MA, USA), p-Akt (1:1,000; CST, MA, USA), t-Akt (1:1,000; CST, MA, USA), p-mTOR (1:1,000; CST, MA, USA), t-mTOR (1:1,000; CST, MA, USA), and β-tubulin (1:1,000; Sungene, Tianjin, China) at 4°C overnight. Then the membranes were reacted with horseradish peroxidase-conjugated secondary antibodies. Chemiluminescence signals were recognized by ECL reagents (Advansta, CA, USA). Blots were quantified with ImageJ software.

### Immunohistochemistry

Kidneys were fixed in 10% formalin and embedded in paraffin. After heat retrieval with heated citrate solution, endogenous peroxidase was blocked by incubation in 0.3% hydrogen peroxide for 10 min. Sections were incubated with primary antibody against SQSTM1/P62 (1:200; Abcam, MA, USA), LC3 (1:200; CST, MA, USA), Col IV (1:200; Proteintech, IL, USA), and FN (1:200; Proteintech, IL, USA) at 4°C overnight. Slides were developed with diaminobenzidine (DAB) kits after incubation with the appropriate secondary antibodies.

### IF

Cells were punched with 1% Triton X-100 after they were fixed with paraformaldehyde. Cells were then blocked with 5% BSA, followed by incubation with primary antibodies against Col IV (1:50; Proteintech, IL, USA), FN (1:5; Proteintech, IL, USA), LC3 (1:50; CST, MA, USA), and SQSTM1/P62 (1:50; CST, MA, USA) at 4°C overnight. After washing with PBS, the cells were incubated with Alexa Fluor-488-conjugated secondary antibodies for 1 hr at room temperature. Nuclei were recognized with DAPI reagents. Fluorescence signals were detected by confocal fluorescence microscopy (Leica Microsystems, Germany).

### RNA Extraction and RT-PCR

Total RNA was extracted from the treated cells with E.Z.N.A. Total RNA Kits (OMEGA, GA, USA). Samples of 1 μg total RNA were reversed with RevertAid First Strand cDNA Synthesis Kits (Thermo, MA, USA) according to the manufacturer's instructions. Real-time qPCR was performed with SYBR Green PCR kits. The primers are listed in Table S2.

### 3-MA Intervention

HMCs were pre-treated for 1 hr with 5 mM 3-MA (Selleck, TX, USA), an inhibitor of autophagy. Then the cells were co-treated with HG (25 mM) and 3-MA, with or without TP for 48 hr.

### Transfection of siRNA

HMCs were transfected with PTEN-siRNA kits (Riobio, Guangzhou, China) or Atg5-siRNA kits (Riobio, Guangzhou, China) using riboFECTTM CP reagent (Riobio, Guangzhou, China), according to the manufacturer's instructions. The PTEN-siRNA sequence was

GAGCGTGCAGATAATGACA and the Atg5-siRNA sequence was GGAATATCCTGCAGAAGAA. Interventions such as HG with or without TP were performed along with transfection for 48 hr.

### Luciferase Reporter Assay

The Mut Express II Fast Mutagenesis Kit V2 (Vazyme, Nanjing, China) was utilized to generate PTEN 3′ UTR mutated versions. HMCs were seeded into 96-well plates for the luciferase reporter assay. Subsequently, the cells were co-transfected with the predicted miR-141-3p binding site and pMIR-PTEN or pMIR-PTEN-mut luciferase reporter. Renilla luciferase was used for normalization. Luciferase activity was evaluated with the Dual-Luciferase Reporter Assay System (Promega, WI, USA) 48 hr after transfection.

### Transfection of miRNA Inhibitor and Mimics

The miR-141-3p inhibitor, miR-141-3p mimics, and the homologous negative control were obtained from GenePharma (Shanghai, China). The cells were transfected with Lipofectamine 2000 reagent (Invitrogen, CA, USA) at the final concentration of 50–100 mM according to the manufacturer's instructions. Treatments were applied to cells 6 hr later.

### Statistical Analysis

Data are expressed as the mean ± SEM. Comparisons between multiple groups were analyzed by one-way ANOVA followed by the Tukey post-test. Statistical significance was determined at $p < 0.05$.

## SUPPLEMENTAL INFORMATION

Supplemental Information includes three figures and two tables and can be found with this article online at http://dx.doi.org/10.1016/j.omtn.2017.08.011.

## AUTHOR CONTRIBUTIONS

B.S. and L.C. conceived and designed the study. X.L., S.W., and Z.H. performed the experiments. Y.Y. and M.X. assisted with analyzing the data. X.L. drafted the manuscript, which was reviewed by F.H. and Y.C.

## CONFLICTS OF INTEREST

The authors declare no competing financial interests.

## ACKNOWLEDGMENTS

This work was supported by the National Natural Science Foundation of China (grants 81273915, 81373864, and 81470187) and the Natural Science Foundation of Tianjin (grants 14JCYBJC26200 and 15ZXHLSY00460).

## REFERENCES

1. Reutens, A.T., and Atkins, R.C. (2011). Epidemiology of diabetic nephropathy. Contrib. Nephrol. *170*, 1–7.
2. Dronavalli, S., Duka, I., and Bakris, G.L. (2008). The pathogenesis of diabetic nephropathy. Nat. Clin. Pract. Endocrinol. Metab. *4*, 444–452.
3. Chen, Z., Siraj, S., Liu, L., and Chen, Q. (2017). MARCH5-FUNDC1 axis fine-tunes hypoxia-induced mitophagy. Autophagy *13*, 1244–1245.
4. Wang, Y., Zhu, W.G., and Zhao, Y. (2017). Autophagy substrate SQSTM1/p62 regulates chromatin ubiquitination during the DNA damage response. Autophagy *13*, 212–213.
5. Zhang, S., Liang, M., Naqvi, N., Lin, C., Qian, W., Zhang, L.H., and Deng, Y.Z. (2017). Phototrophy and starvation-based induction of autophagy upon removal of Gcn5-catalyzed acetylation of Atg7 in Magnaporthe oryzae. Autophagy, Published online June 8, 2017. http://dx.doi.org/10.1080/15548627.2017.1327103.
6. Gretzmeier, C., Eiselein, S., Johnson, G.R., Engelke, R., Nowag, H., Zarei, M., Küttner, V., Becker, A.C., Rigbolt, K.T.G., Høyer-Hansen, M., et al. (2017). Degradation of protein translation machinery by amino acid starvation-induced macroautophagy. Autophagy *13*, 1064–1075.
7. Kitada, M., Ogura, Y., Monno, I., and Koya, D. (2017). Regulating autophagy as a therapeutic target for diabetic nephropathy. Curr. Diab. Rep. *17*, 53.
8. Forbes, M.S., Thornhill, B.A., and Chevalier, R.L. (2011). Proximal tubular injury and rapid formation of atubular glomeruli in mice with unilateral ureteral obstruction: a new look at an old model. Am. J. Physiol. Renal Physiol. *301*, F110–F117.
9. Xu, Y., Ruan, S., Wu, X., Chen, H., Zheng, K., and Fu, B. (2013). Autophagy and apoptosis in tubular cells following unilateral ureteral obstruction are associated with mitochondrial oxidative stress. Int. J. Mol. Med. *31*, 628–636.
10. Kolling, M., Kaucsar, T., Schauerte, C., Hubner, A., Dettling, A., Park, J.K., Busch, M., Wulff, X., Meier, M., Scherf, K., and Bukosza, N. (2017). Therapeutic miR-21 silencing ameliorates diabetic kidney disease in mice. Mol. Ther. *25*, 165–180.
11. Zanchi, C., Macconi, D., Trionfini, P., Tomasoni, S., Rottoli, D., Locatelli, M., Rudnicki, M., Vandesompele, J., Mestdagh, P., Remuzzi, G., et al. (2017). MicroRNA-184 is a downstream effector of albuminuria driving renal fibrosis in rats with diabetic nephropathy. Diabetologia *60*, 1114–1125.
12. Kato, M., Dang, V., Wang, M., Park, J.T., Deshpande, S., Kadam, S., Mardiros, A., Zhan, Y., Oettgen, P., Putta, S., et al. (2013). TGF-β induces acetylation of chromatin and of Ets-1 to alleviate repression of miR-192 in diabetic nephropathy. Sci. Signal. *6*, ra43.
13. Chen, C., Yang, S., Zhang, M., Zhang, Z., Zhang, S.B., Wu, B., Hong, J., Zhang, W., Lin, J., Okunieff, P., and Zhang, L. (2017). Triptolide mitigates radiation-induced pneumonitis via inhibition of alveolar macrophages and related inflammatory molecules. Oncotarget *8*, 45133–45142.
14. Song, J.M., Molla, K., Anandharaj, A., Cornax, I., O Sullivan, M.G., Kirtane, A.R., Panyam, J., and Kassie, F. (2017). Triptolide suppresses the in vitro and in vivo growth of lung cancer cells by targeting hyaluronan-CD44/RHAMM signaling. Oncotarget *8*, 26927–26940.
15. Zhang, L.Y., Li, H., Wu, Y.W., Cheng, L., Yan, Y.X., Yang, X.Q., Zhu, F.H., He, S.J., Tang, W., and Zuo, J.P. (2017). (5R)-5-hydroxytriptolide ameliorates lupus nephritis in MRL/lpr mice by preventing infiltration of immune cells. Am. J. Physiol. Renal Physiol. *312*, F769–F777.
16. Guo, X., Xue, M., Li, C.J., Yang, W., Wang, S.S., Ma, Z.J., Zhang, X.N., Wang, X.Y., Zhao, R., Chang, B.C., and Chen, L.M. (2016). Protective effects of triptolide on TLR4 mediated autoimmune and inflammatory response induced myocardial fibrosis in diabetic cardiomyopathy. J. Ethnopharmacol. *193*, 333–344.
17. Zhu, B., Wang, Y., Jardine, M., Jun, M., Lv, J.C., Cass, A., Liyanage, T., Chen, H.Y., Wang, Y.J., and Perkovic, V. (2013). Tripterygium preparations for the treatment of CKD: a systematic review and meta-analysis. Am. J. Kidney Dis. *62*, 515–530.
18. Ge, Y., Xie, H., Li, S., Jin, B., Hou, J., Zhang, H., Shi, M., and Liu, Z. (2013). Treatment of diabetic nephropathy with Tripterygium wilfordii Hook F extract: a prospective, randomized, controlled clinical trial. J. Transl. Med. *11*, 134.
19. Gao, Q., Shen, W., Qin, W., Zheng, C., Zhang, M., Zeng, C., Wang, S., Wang, J., Zhu, X., and Liu, Z. (2010). Treatment of db/db diabetic mice with triptolide: a novel therapy for diabetic nephropathy. Nephrol. Dial. Transplant. *25*, 3539–3547.
20. Guo, H., Pan, C., Chang, B., Wu, X., Guo, J., Zhou, Y., Liu, H., Zhu, Z., and Chen, L. (2016). Triptolide improves diabetic nephropathy by regulating Th cell balance and macrophage infiltration in rat models of diabetic nephropathy. Exp. Clin. Endocrinol. Diabetes *124*, 389–398.
21. Ma, R., Liu, L., Liu, X., Wang, Y., Jiang, W., and Xu, L. (2013). Triptolide markedly attenuates albuminuria and podocyte injury in an animal model of diabetic nephropathy. Exp. Ther. Med. *6*, 649–656.

22. Ma, Z.J., Zhang, X.N., Li, L., Yang, W., Wang, S.S., Guo, X., Sun, P., and Chen, L.M. (2015). Tripterygium glycosides tablet ameliorates renal tubulointerstitial fibrosis via the Toll-Like receptor 4/nuclear factor kappa B signaling pathway in high-fat diet fed and streptozotocin-induced diabetic rats. J. Diabetes Res. *2015*, 390428.

23. Miller, C.G., Pozzi, A., Zent, R., and Schwarzbauer, J.E. (2014). Effects of high glucose on integrin activity and fibronectin matrix assembly by mesangial cells. Mol. Biol. Cell *25*, 2342–2350.

24. Ding, Y., and Choi, M.E. (2014). Regulation of autophagy by TGF-β: emerging role in kidney fibrosis. Semin. Nephrol. *34*, 62–71.

25. Ding, Y., Kim, Sl., Lee, S.Y., Koo, J.K., Wang, Z., and Choi, M.E. (2014). Autophagy regulates TGF-β expression and suppresses kidney fibrosis induced by unilateral ureteral obstruction. J. Am. Soc. Nephrol. *25*, 2835–2846.

26. Poncelet, A.C., de Caestecker, M.P., and Schnaper, H.W. (1999). The transforming growth factor-beta/SMAD signaling pathway is present and functional in human mesangial cells. Kidney Int. *56*, 1354–1365.

27. Inoki, K., Haneda, M., Ishida, T., Mori, H., Maeda, S., Koya, D., Sugimoto, T., and Kikkawa, R. (2000). Role of mitogen-activated protein kinases as downstream effectors of transforming growth factor-β in mesangial cells. Kidney Int. Suppl. *77*, S76–S80.

28. Chin, B.Y., Mohsenin, A., Li, S.X., Choi, A.M., and Choi, M.E. (2001). Stimulation of pro-alpha(1)(I) collagen by TGF-beta(1) in mesangial cells: role of the p38 MAPK pathway. Am. J. Physiol. Renal Physiol. *280*, F495–F504.

29. Kim, S.I., Na, H.J., Ding, Y., Wang, Z., Lee, S.J., and Choi, M.E. (2012). Autophagy promotes intracellular degradation of type I collagen induced by transforming growth factor (TGF)-β1. J. Biol. Chem. *287*, 11677–11688.

30. Klionsky, D.J., Abdelmohsen, K., Abe, A., Abedin, M.J., Abeliovich, H., Acevedo Arozena, A., Adachi, H., Adams, C.M., Adams, P.D., Adeli, K., and Adhihetty, P.J. (2016). Guidelines for the use and interpretation of assays for monitoring autophagy. Autophagy *12*, 1–222.

31. Zhan, M., Usman, I.M., Sun, L., and Kanwar, Y.S. (2015). Disruption of renal tubular mitochondrial quality control by Myo-inositol oxygenase in diabetic kidney disease. J. Am. Soc. Nephrol. *26*, 1304–1321.

32. Kroemer, G., Mariño, G., and Levine, B. (2010). Autophagy and the integrated stress response. Mol. Cell *40*, 280–293.

33. Hu, G., Gong, X., Wang, L., Liu, M., Liu, Y., Fu, X., Wang, W., Zhang, T., and Wang, X. (2017). Triptolide promotes the clearance of α-synuclein by enhancing autophagy in neuronal cells. Mol. Neurobiol. *54*, 2361–2372.

34. Zhao, F., Huang, W., Zhang, Z., Mao, L., Han, Y., Yan, J., and Lei, M. (2016). Triptolide induces protective autophagy through activation of the CaMKKβ-AMPK signaling pathway in prostate cancer cells. Oncotarget *7*, 5366–5382.

35. Maehama, T., and Dixon, J.E. (1998). The tumor suppressor, PTEN/MMAC1, dephosphorylates the lipid second messenger, phosphatidylinositol 3,4,5-trisphosphate. J. Biol. Chem. *273*, 13375–13378.

36. Miao, B., Skidan, I., Yang, J., Lugovskoy, A., Reibarkh, M., Long, K., Brazell, T., Durugkar, K.A., Maki, J., Ramana, C.V., et al. (2010). Small molecule inhibition of phosphatidylinositol-3,4,5-triphosphate (PIP3) binding to pleckstrin homology domains. Proc. Natl. Acad. Sci. USA *107*, 20126–20131.

37. Pullen, N., Dennis, P.B., Andjelkovic, M., Dufner, A., Kozma, S.C., Hemmings, B.A., and Thomas, G. (1998). Phosphorylation and activation of p70s6k by PDK1. Science *279*, 707–710.

38. Inoki, K., Li, Y., Zhu, T., Wu, J., and Guan, K.L. (2002). TSC2 is phosphorylated and inhibited by Akt and suppresses mTOR signalling. Nat. Cell Biol. *4*, 648–657.

39. Inoki, K., Li, Y., Xu, T., and Guan, K.L. (2003). Rheb GTPase is a direct target of TSC2 GAP activity and regulates mTOR signaling. Genes Dev. *17*, 1829–1834.

40. Sancak, Y., Thoreen, C.C., Peterson, T.R., Lindquist, R.A., Kang, S.A., Spooner, E., Carr, S.A., and Sabatini, D.M. (2007). PRAS40 is an insulin-regulated inhibitor of the mTORC1 protein kinase. Mol. Cell *25*, 903–915.

41. Hosokawa, N., Hara, T., Kaizuka, T., Kishi, C., Takamura, A., Miura, Y., Iemura, S., Natsume, T., Takehana, K., Yamada, N., et al. (2009). Nutrient-dependent mTORC1 association with the ULK1-Atg13-FIP200 complex required for autophagy. Mol. Biol. Cell *20*, 1981–1991.

42. Kim, J., Kundu, M., Viollet, B., and Guan, K.L. (2011). AMPK and mTOR regulate autophagy through direct phosphorylation of Ulk1. Nat. Cell Biol. *13*, 132–141.

43. Hur, K., Toiyama, Y., Takahashi, M., Balaguer, F., Nagasaka, T., Koike, J., Hemmi, H., Koi, M., Boland, C.R., and Goel, A. (2013). MicroRNA-200c modulates epithelial-to-mesenchymal transition (EMT) in human colorectal cancer metastasis. Gut *62*, 1315–1326.

44. Liu, C., Liu, R., Zhang, D., Deng, Q., Liu, B., Chao, H.P., Rycaj, K., Takata, Y., Lin, K., Lu, Y., et al. (2017). MicroRNA-141 suppresses prostate cancer stem cells and metastasis by targeting a cohort of pro-metastasis genes. Nat. Commun. *8*, 14270.

45. Ho, B.C., Yu, S.L., Chen, J.J., Chang, S.Y., Yan, B.S., Hong, Q.S., Singh, S., Kao, C.L., Chen, H.Y., Su, K.Y., et al. (2011). Enterovirus-induced miR-141 contributes to shutoff of host protein translation by targeting the translation initiation factor eIF4E. Cell Host Microbe *9*, 58–69.

46. Wang, B., Koh, P., Winbanks, C., Coughlan, M.T., McClelland, A., Watson, A., Jandeleit-Dahm, K., Burns, W.C., Thomas, M.C., Cooper, M.E., and Kantharidis, P. (2011). miR-200a prevents renal fibrogenesis through repression of TGF-β2 expression. Diabetes *60*, 280–287.

47. Baseler, W.A., Thapa, D., Jagannathan, R., Dabkowski, E.R., Croston, T.L., and Hollander, J.M. (2012). miR-141 as a regulator of the mitochondrial phosphate carrier (Slc25a3) in the type 1 diabetic heart. Am. J. Physiol. Cell Physiol. *303*, C1244–C1251.

48. Xiong, M., Jiang, L., Zhou, Y., Qiu, W., Fang, L., Tan, R., Wen, P., and Yang, J. (2012). The miR-200 family regulates TGF-β1-induced renal tubular epithelial to mesenchymal transition through Smad pathway by targeting ZEB1 and ZEB2 expression. Am. J. Physiol. Renal Physiol. *302*, F369–F379.